

Article

Edaphic Determinants of Biomass Hyperdominance in Large Trees of the Amazon

Manuelle Pereira ^{1,*} , Jorge Luis Reategui-Betancourt ² , Robson de Lima ² , Paulo Bittencourt ³ , Eric Gorgens ⁴ , Gustavo Abreu ² , Marcelino Guedes ⁵ , José Silva ¹, Carla de Sousa ², Joselane Priscila da Silva ² , Elisama de Souza ¹  and Diego Armando Silva ¹ 

¹ Campus Laranjal do Jari, Instituto Federal de Educação, Ciência e Tecnologia do Amapá (IFAP), Laranjal do Jari 68920-000, AP, Brazil; diego.armando@ifap.edu.br (D.A.S.)

² Laboratório de Manejo Florestal, Universidade do Estado do Amapá, Macapá 68901-262, AP, Brazil; jorgereategui91@gmail.com (J.L.R.-B.)

³ School of Earth and Environment Sciences, Cardiff University, Cardiff CF10 3AT, UK

⁴ Departamento de Engenharia Florestal, Universidade Federal dos Vales do Jequitinhonha e Mucuri, Diamantina 39100-000, MG, Brazil

⁵ Empresa Brasileira de Pesquisa Agropecuária, Macapá 68903-419, AP, Brazil

* Correspondence: cmanu043@gmail.com

Abstract

Amazonian large trees act as central elements of forest ecosystems, storing a disproportionate fraction of aboveground biomass. However, these trees are not randomly distributed across the landscape, and it is expected that edaphic attributes influence floristic composition, forest structure, and vegetation biomass. In this study, we investigated how variation in soil chemical and physical properties affects the diversity and biomass of large trees. Forest inventories were conducted at five sites within protected areas in the states of Pará and Amapá. Aboveground biomass was estimated using allometric equations, while soil samples were analyzed for their physical and chemical properties. Diversity indices, rarefaction, Redundancy Analysis, and Generalized Additive Models were applied. Edaphic variables such as soil pH, organic matter, phosphorus, and aluminum were associated with floristic composition and the biomass of these individuals. Trees with a diameter at breast height greater than or equal to 70 cm accounted for up to 80% of total biomass, revealing a pattern of biomass hyperdominance. The results indicate that the occurrence of large trees is related to edaphic and structural attributes, such as tree density and size distribution, suggesting that these individuals are not randomly distributed along soil gradients. Understanding these patterns is essential for improving ecological models, biomass extrapolations, and management strategies aimed at conserving the Amazon rainforest.

Keywords: Amazon basin; forest biomass; forest conservation; large trees; soil–vegetation interactions



Academic Editor: José Aranha

Received: 15 November 2025

Revised: 31 December 2025

Accepted: 6 January 2026

Published: 16 March 2026

Copyright: © 2026 by the authors.

Licensee MDPI, Basel, Switzerland.

This article is an open access article distributed under the terms and

conditions of the [Creative Commons](https://creativecommons.org/licenses/by/4.0/)

[Attribution \(CC BY\)](https://creativecommons.org/licenses/by/4.0/) license.

1. Introduction

The Amazon, the largest continuous tropical forest on the planet, harbors unparalleled biological and structural diversity shaped by complex interactions among stable climate, high water availability, and heterogeneous edaphic gradients [1,2]. Together, these factors support highly specialized plant communities, including mega-trees that stand out not only for their exceptional dimensions but also for their central role in ecological and climatic regulation [3].

Within the Amazonian landscape, large trees [4] are defined as individuals with a diameter at breast height (DBH) ≥ 70 cm [5]. These individuals hold cultural significance for local communities, perform essential ecological functions, and sustain a wide range of associated organisms [3]. They also store a substantial portion of forest biomass, playing a critical role in carbon storage and in maintaining forest structural integrity [6]. This DBH threshold has been widely adopted in studies of forest structure and biomass distribution in tropical ecosystems and in global monitoring networks, as well as in the protocol proposed by Harris et al. [7] for forest research in the Republic of the Congo. Recent surveys in the Amazon [6] also employ this threshold, which marks the size class above which individuals begin to concentrate a disproportionate fraction of total aboveground biomass [8,9]. This standardized definition facilitates comparisons among studies and reinforces the functional importance of large trees in sustaining carbon stocks and forest structure.

Recent studies have identified regions with high concentrations of giant trees in the states of Pará and Amapá, Brazil [6,10]. This region encompasses pronounced gradients of geomorphological units, soil types, and hydrological conditions, making it an ecologically strategic setting for investigating the drivers of large-tree occurrence [2,6,11]. Ecologically, these trees function as “ecosystem engineers,” influencing both the structure and diversity of plant communities, while contributing disproportionately to aboveground biomass and carbon stocks [3,6]. Their role in carbon storage further underscores their relevance in the context of climate change [6,10].

Large trees account for a significant proportion of aboveground biomass in tropical forests, exemplifying the phenomenon of biomass hyperdominance, described by Slik et al. [8], whereby a small number of individuals or species are responsible for a disproportionate share of carbon storage. This pattern is consistently observed across Amazonian forests [12], and is supported by pantropical evidence showing that approximately 1% of species can contain up to half of total biomass and carbon productivity [13]. From a functional perspective, trees with DBH ≥ 60 –70 cm may represent between one-third and nearly half of living biomass [9,14], thereby acting as structural keystones for forest stability and carbon storage in tropical forests.

Despite their ecological importance, the environmental conditions that enable the establishment, persistence, and growth of these large trees remain poorly understood, particularly with respect to edaphic controls. Soil physical and chemical properties are major determinants of tropical forest structure, as they regulate nutrient availability, water retention, root development, and interspecific competition [2]. However, large areas of the Amazon remain scientifically unexplored, limiting our understanding of its ecological heterogeneity [15]. This knowledge gap is especially pronounced in eastern Amazonia, where complex soil mosaics prevail and the role of edaphic heterogeneity in shaping forest biomass distribution and large-tree dominance remains unresolved.

In this study, we evaluate whether edaphic heterogeneity is associated with spatial variation in the occurrence, diversity, and aboveground biomass of large trees (DBH ≥ 70 cm) across eastern Amazonia. Specifically, we test the hypothesis that variation in soil physical and chemical properties is statistically associated with both the diversity and the aboveground biomass of large-sized individuals.

2. Materials and Methods

2.1. Description and Location of the Study Area

This study was conducted at five sites with a high occurrence of giant trees in the northern Amazon region, located in the states of Amapá and Pará, Brazil (AG, Urucupatá, Ipitinga, Iratapuru, and Cupixi). These sites were selected based on recent large-scale assessments identifying eastern Amazonia, particularly Pará and Amapá, as regions with

some of the highest densities of giant trees across the Amazon basin [6]. In addition, all study sites are located within legally protected areas, which allowed the establishment and long-term maintenance of permanent forest plots.

Although the selected sites do not aim to represent the entire Amazon region, they encompass environmentally heterogeneous landscapes within a recognized giant-tree hotspot. Forest inventory and soil data were collected and analyzed between 2019 and 2024. Three of the study sites are located within the Environmental State Park of the Giant Trees of the Amazon ($0^{\circ}41'29''$ N, $53^{\circ}28'41''$ W), and two sites are situated in the Rio Iratapuru Sustainable Development Reserve ($0^{\circ}19'05''$ N, $52^{\circ}43'29''$ W) (Figure 1).

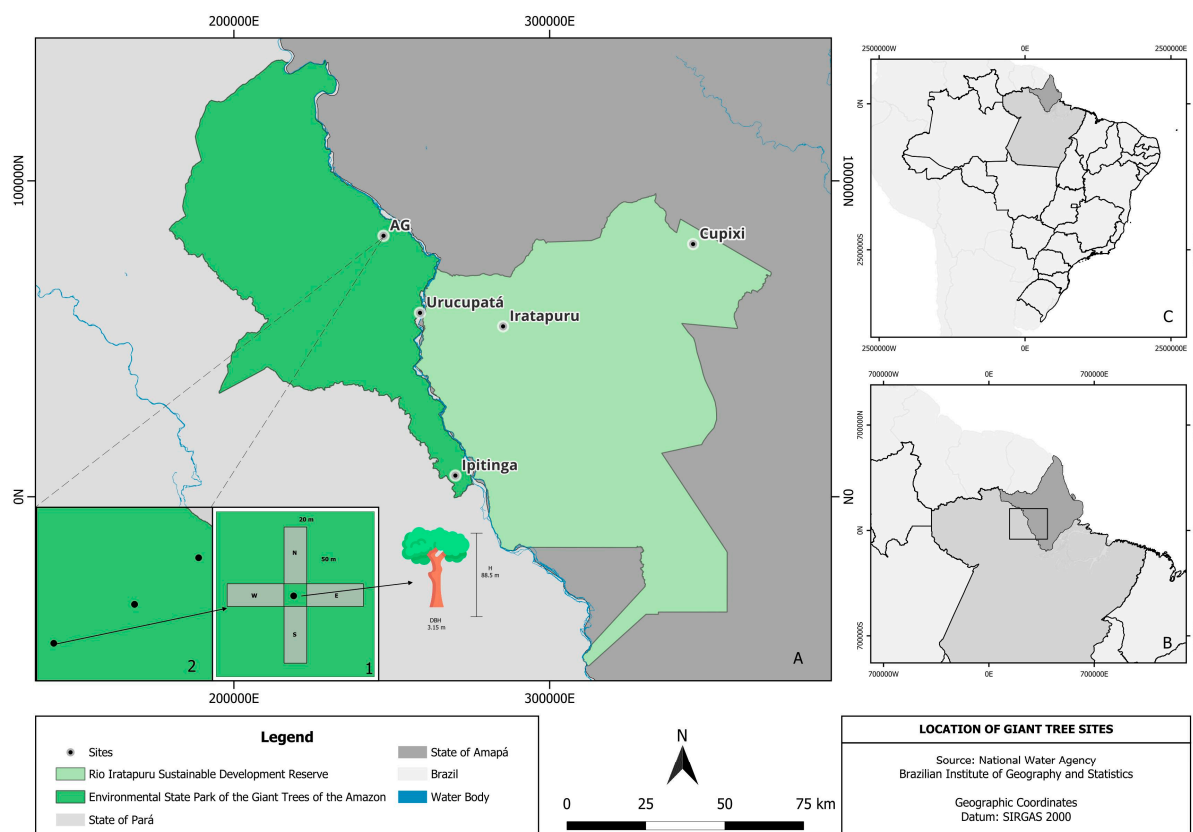


Figure 1. Location and sampling design of the study areas in the Eastern Amazon, Brazil. (A) Delimitation of the protected study areas, represented by different colors according to the legend in the figure, including the Environmental State Park of the Giant Trees of the Amazon and the Rio Iratapuru Sustainable Development Reserve. (1) Schematic representation of the sampling design, illustrating the delineation of the sampling clusters centered on a reference giant tree and the orientation of the subplots along the cardinal directions. (2) Spatial arrangement of the sampling clusters within each study area. (B) Regional reference map indicating the location of the study areas in northern Brazil (black frame). (C) Map of Brazil showing the geographic context of the study region within South America.

Both areas are situated within the domain of Amazonian dense ombrophilous forest, under a climate classified as Af (Köppen), characterized by a humid equatorial regime with abundant rainfall throughout the year, mean annual temperatures above 25°C , and total annual precipitation generally exceeding 2500 mm [16].

2.2. Data Collection

2.2.1. Floristic Inventory

At each study site, a cluster-based sampling design (conglomerate sampling) was adopted. Three sampling clusters were established per site, each centered on a giant tree serving as the central reference point (Figure 1A). Each cluster was composed of four rectangular subplots arranged in the four cardinal directions (north, east, south, and west), each measuring 20 × 50 m (1.000 m²; 0.1 ha).

This design resulted in 12 subplots per site and a total sampled area of 1.2 ha per site, summing to 6.0 ha across the five study sites. The use of 20 × 50 m subplots follows the methodological guidelines of the Brazilian Forest Service (SFB/IFN) [17] and represents an operationally efficient and scientifically robust sampling strategy for Amazonian forests, particularly under conditions of limited accessibility and complex terrain. When applied within a clustered design centered on large trees, this subplot size ensures adequate representation of forest structure and aboveground biomass while maintaining field feasibility.

All woody individuals with a diameter at breast height (DBH) ≥ 10 cm were measured, a threshold widely adopted in tropical forest inventories focused on forest structure and aboveground biomass estimation. Tree height was estimated using a hypsometer, except for the giant trees serving as central references for the clusters, whose heights were obtained from LiDAR (Light Detection and Ranging) data [10]. Smaller diameter classes were not included in the analyses because they tend to contribute less to total biomass and are more commonly used to investigate forest dynamics and regeneration processes, which, although addressed in complementary studies, were not the primary focus of this work.

Botanical identification was performed with the assistance of experienced local parataxonomists, based on dendrological characteristics such as leaves, crown shape, trunk, and bark. Scientific names and families were validated using the Flora and Funga of Brazil database (<https://reflora.jbrj.gov.br/reflora/>, accessed on 6 August 2025). The geographic coordinates of each tree were recorded using a GPS receiver (Garmin 65 CSx; Garmin Ltd., Olathe, KS, USA; manufactured in Taiwan).

2.2.2. Soil Sampling and Analysis

Soil sampling followed EMBRAPA guidelines, which recommend a minimum of eight subsamples per subplot combined into a representative composite sample [18]. Each subplot was subdivided into quadrants of 25 m², from which eight were systematically selected for soil sampling in the 0–20 cm layer. The simple samples were homogenized to form a composite sample representative of each subplot [19]. Physical and chemical analyses were conducted at the EMBRAPA Soil Laboratories of Amapá and Pará, following the protocols established by [20].

2.2.3. Biomass Calculation

Biomass estimation was performed using regional allometric models implemented in the BIOMASS package (version 2.2.4-1) [21]. The equation followed the allometric model developed by Chave et al. [22], which incorporates as independent variables the diameter at breast height (DBH, in cm), tree height (H, in m), and wood density (WD, in g/cm³), expressed as:

$$AGB = 0.0673 \times (WD \times DBH^2 \times H)^{0.976}, \quad (1)$$

where AGB represents the aboveground biomass of each tree (in kg). The total biomass of each sampling unit was converted to biomass per area (Mg/ha), considering the effective sampled area in each plot.

2.2.4. Data Analysis

To assess the relationship between the biomass of trees with $DBH \geq 70$ cm, overall floristic diversity (species richness and Shannon index), and forest structure (individual density (individuals ha^{-1})), Spearman's rank correlation coefficient was applied.

To investigate the association between floristic composition and edaphic attributes across sites, a Redundancy Analysis (RDA) was performed. This multivariate ordination technique combines elements of Principal Component Analysis and multiple linear regression [23], allowing multiple soil attributes to be evaluated simultaneously as explanatory variables, while assessing their individual contributions to the variation in floristic composition among plots. The tree species abundance matrix was constructed based on counts of woody individuals per plot and transformed using the Hellinger method [24].

Continuous edaphic variables were standardized (mean = 0, standard deviation = 1) to ensure comparability among scales. To reduce multicollinearity among predictors, a forward selection procedure based on statistical significance ($p < 0.05$) was applied using the `forward.sel` function from the `adespatial` package (version 0.3-28) [25]. The RDA was conducted using the `rda()` function of the `vegan` package (version 2.7-2) [26]. The significance of canonical axes and individual predictor variables was tested using permutation tests (999 iterations). The adjusted coefficient of determination (adjusted R^2) was used to quantify the explanatory power of the model.

To evaluate whether the physical and chemical characteristics of the plots' soils influenced the variation in large-tree biomass, a Generalized Linear Model (GLM) with Gamma distribution and log link function was initially fitted, which is suitable for continuous and strictly positive data. From the full model, edaphic variables were selected through a bidirectional stepwise procedure based on the Akaike Information Criterion (AIC), in order to reduce collinearity among predictors and avoid model overfitting [27]. The functions `glm()` and `step()` from the `stats` package (version 4.5.2) [28] were used.

The variables selected through the stepwise procedure were subsequently employed to fit a Generalized Additive Model (GAM) with Gaussian family, which incorporates smoothing functions (splines) to model nonlinear relationships between soil attributes and tree biomass [29]. This approach does not impose a rigid functional form on the relationships, providing greater flexibility for describing complex ecological patterns [30]. The model was fitted using the `gam()` function of the `mgcv` package (version 1.9-4) [29]. The analysis considered only plots with positive biomass values of large trees, excluding 17 plots with zero values to satisfy the assumptions of the Gamma distribution and focus inference on areas with the actual presence of these trees.

3. Results

A total of 101 large-sized tree individuals ($DBH \geq 70$ cm) were recorded in the sampled areas, representing 52 species distributed across 21 families, with one individual not identified. These individuals exhibited DBH values ranging from 70.03 to 321.49 cm and heights between 11 and 79 m. Individual biomass ranged from approximately 0.002 to 0.209 Mg. A summary of the structural attributes of these individuals is presented in Table A1.

The results indicate that biomass, particularly that of large trees, depends more strongly on the abundance of these individuals ($r = 0.75$, $p < 0.001$) than on overall floristic diversity (Figure 2). This outcome is expected, as biomass accumulation is directly related to the number of large-sized individuals present. A strong correlation was also observed between the biomass of large trees and the total forest biomass ($r = 0.99$, $p < 0.001$), demonstrating that a small number of large trees concentrate a substantial proportion of the total biomass stock across the evaluated sites.

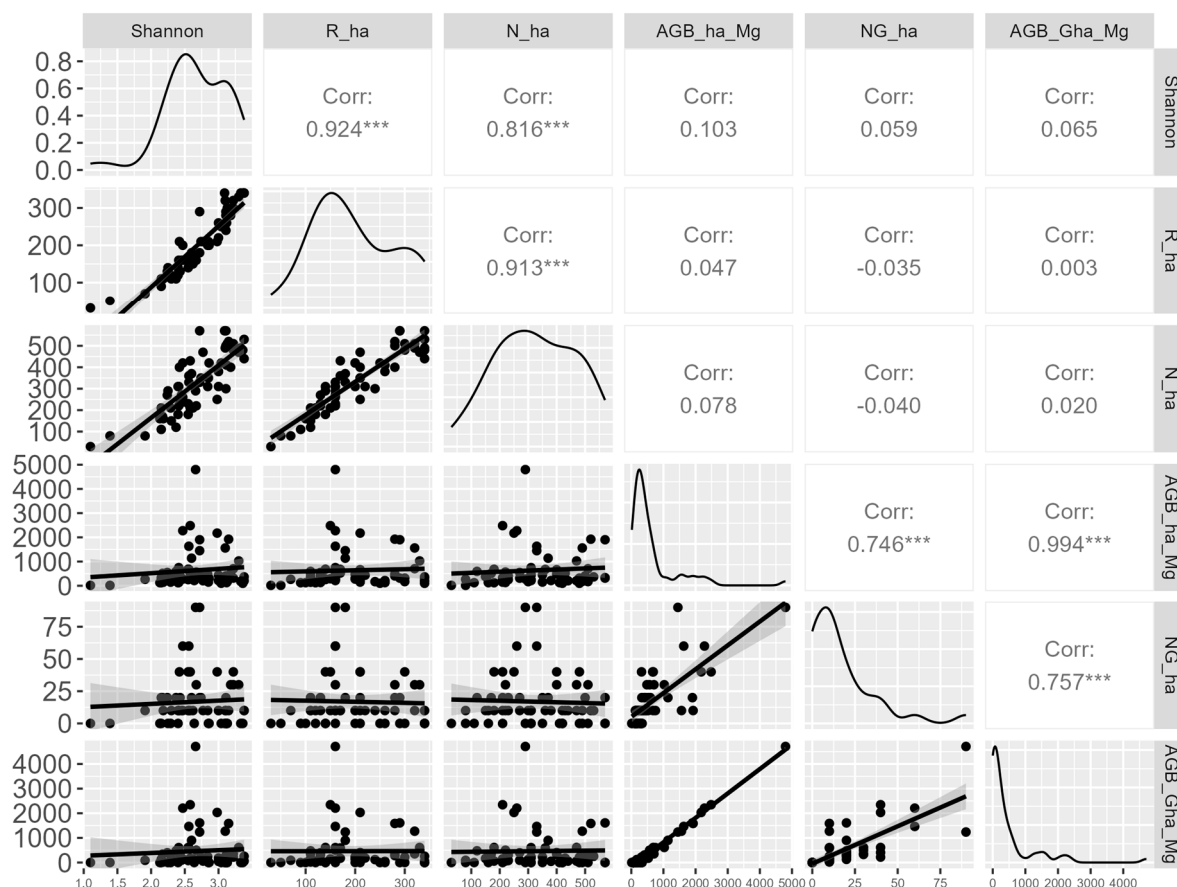


Figure 2. Correlations among the Shannon diversity index, total species richness per hectare (R_{ha}), total tree density per hectare (N_{ha}), total aboveground biomass per hectare (AGB_{ha_Mg} ; $Mg\ ha^{-1}$), density of large trees per hectare (NG_{ha}), and aboveground biomass of large trees per hectare (AGB_{Gha_Mg} ; $Mg\ ha^{-1}$) in giant-tree sites of the Eastern Amazon (Pará and Amapá, Brazil). Significance levels are indicated as follows: *** $p < 0.001$.

Biomass hyperdominance was driven by a small number of species. Across all sites, six species accounted for a disproportionate share of aboveground biomass per hectare among trees: *Swartzia polyphylla* ($n = 1$), *Dinizia excelsa* ($n = 4$), *Inga auristellae* ($n = 2$), *Terminalia amazonia* ($n = 3$), *Inga* sp. ($n = 4$) and *Bertholletia excelsa* ($n = 6$) (Table A1). Although represented by few individuals, these species contributed substantially to total biomass, highlighting the species-specific nature of biomass hyperdominance. This pattern is further illustrated by the site-level distribution of aboveground biomass, which shows the disproportionate contribution of a small number of large individuals to total biomass (Figure A1).

To further explore the environmental drivers of species composition, the Redundancy Analysis (RDA) revealed that six edaphic variables, potential acidity ($H^+ + Al^{3+}$), fine sand content, potassium (K^+), aluminum (Al^{3+}), total sand, and soil organic matter (SOM), jointly explained 21.5% of the variation in tree species composition (Figure 3), with an adjusted R^2 of 12.6%. The canonical axes (RDA1 and RDA2) represent the main edaphic gradients among plots. RDA1 was associated with lower concentrations of $H^+ + Al^{3+}$ and SOM, and higher levels of Al^{3+} , K^+ , total sand, and fine sand. In contrast, RDA2 was related to higher concentrations of $H^+ + Al^{3+}$ and Al^{3+} , and lower values of SOM, K^+ , fine sand, and total sand.

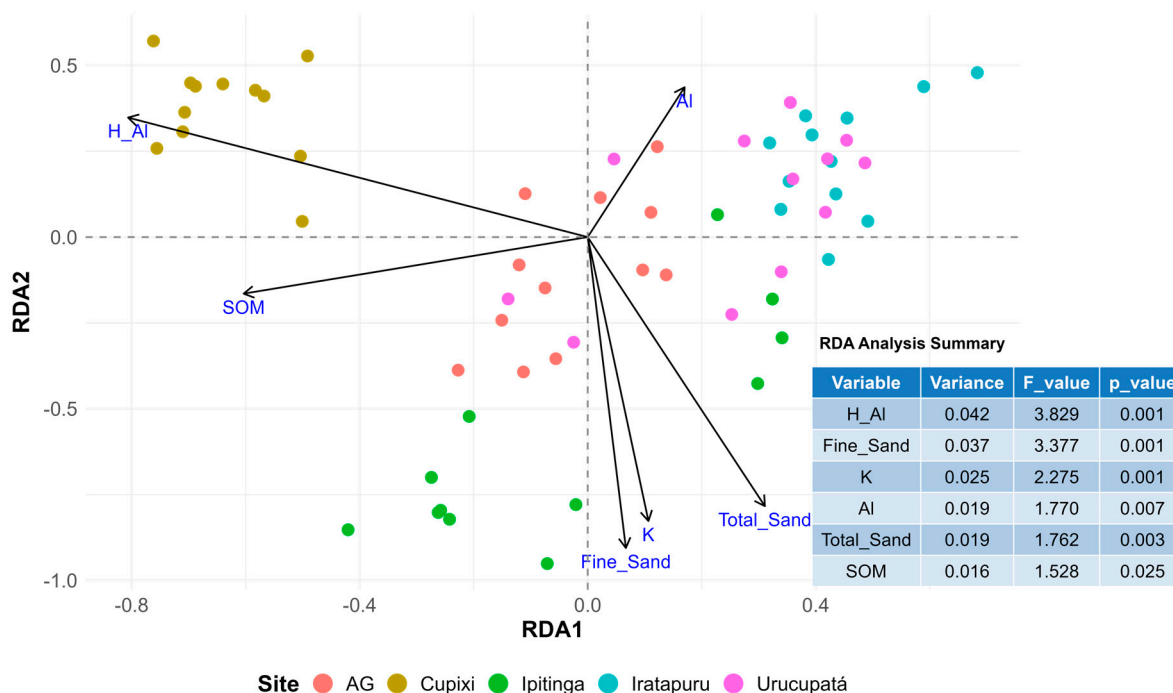


Figure 3. Redundancy Analysis (RDA) of floristic composition as a function of edaphic variables in Amazonian sites located in the states of Pará and Amapá, Brazil. The ordination is based on a Hellinger-transformed tree species abundance matrix. The associated table summarizes the edaphic variables retained by the forward selection procedure, including the proportion of explained variance, F-values, and P-values for each attribute. H_Al = potential acidity ($H^+ + Al^{3+}$); Fine Sand = fine sand; K = potassium (K^+); Al = aluminum (Al^{3+}); Total Sand = total sand; and SOM = soil organic matter.

All selected variables were significant in the analysis, according to permutation tests from the RDA forward selection procedure, indicating the presence of environmental gradients affecting tree species composition. Among the analyzed sites, Cupixi stood out for its strong association with the potential acidity gradient ($H^+ + Al^{3+}$), positioned at the negative extreme of the RDA1 axis. All selected variables showed individual statistical significance, reinforcing that edaphic factors play a key role in shaping the floristic structure and composition of the studied area.

The Generalized Additive Model (GAM) indicated significant nonlinear effects of soil pH, soil organic matter (SOM), phosphorus (P), and aluminum (Al^{3+}) on the biomass of large trees ($DBH \geq 70$ cm), with varying degrees of smoothness and statistical support (Table A4). The model explained 74.6% of the total variance (adjusted pseudo- $R^2 = 0.631$), demonstrating a good fit to the data (Figure 4).

Nonlinear GAM responses revealed clear functional ranges for key soil variables (Table A5). Large-tree biomass increased within a soil pH range of approximately 3.52–6.17, indicating optimal slightly to moderately acidic conditions. Biomass also showed a positive marginal response to phosphorus availability between 1.60 and 6.50 $mg\ kg^{-1}$, after which the response tended to stabilize rather than decline. Aluminum exhibited a positive effect within an intermediate range (0.73–1.42 $cmolc\ kg^{-1}$), suggesting a tolerance window characteristic of species adapted to acidic Amazonian soils, rather than a simple toxicity threshold. Soil organic matter did not exhibit a well-defined threshold or monotonic response, indicating a weak or non-linear influence on large-tree biomass.

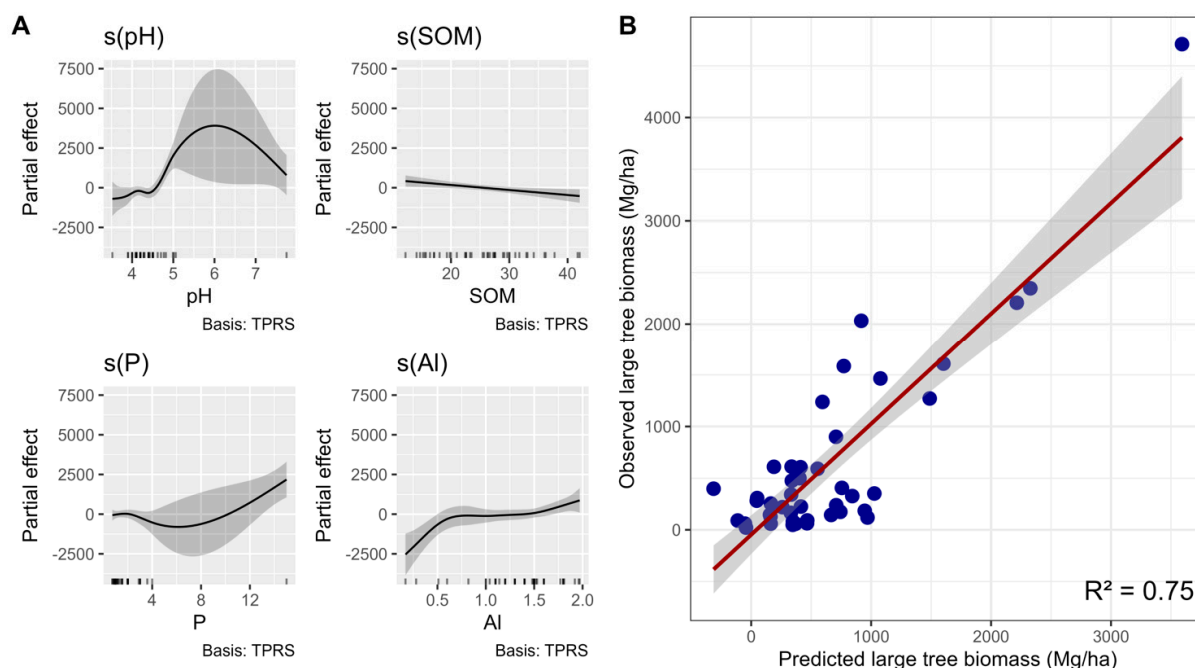


Figure 4. Smoothed effects of the edaphic variables pH ($p = 0.00107$), SOM ($p = 0.01410$), P ($p = 0.00426$), and Al ($p = 0.00235$) on the biomass of large trees (DBH ≥ 70 cm) in the Eastern Amazon, according to the Generalized Additive Model (GAM) fitted for the states of Pará and Amapá, Brazil. (A) displays the nonlinear effects of each soil attribute on biomass (Mg ha^{-1}), while (B) shows the relationship between observed and predicted values. The red line represents the values predicted by the GAM, and the gray shaded area indicates the 95% confidence interval. The model explained 74.6% of the total variance (adjusted pseudo- $R^2 = 0.631$).

4. Discussion

4.1. Edaphic Controls on Large-Tree Biomass

Total biomass was strongly associated with the abundance of large trees, confirming the pattern of biomass hyperdominance in the Amazon [8]. This phenomenon reflects the disproportionate contribution of a small number of individuals to total biomass stocks, indicating that emergent trees play a central structural role in the stability and functioning of the ecosystem [14,30]. In some sites, a single individual accounted for up to 82% of living biomass, supporting previous studies that emphasize the importance of large trees as key carbon reservoirs and regulators of forest dynamics [6].

Potential acidity, fine sand, potassium, aluminum, total sand, and soil organic matter explained a statistically significant but moderate proportion of variation in floristic composition (Figure 3). Although the amount of variance explained by the RDA was relatively low, this outcome is expected in highly diverse tropical forests, where strong environmental heterogeneity, stochastic demographic processes, and unmeasured biotic interactions constrain the explanatory power of constrained ordination methods. Within this context, the detected edaphic gradients represent dominant axes of environmental filtering rather than exhaustive drivers of community structure.

This pattern reflects the intrinsically low fertility of most Amazonian soils [31], which limits both diversity and growth, consistent with studies highlighting the direct influence of edaphic properties on species composition and distribution [11,32,33]. The strong association of the Cupixi site with potential acidity ($\text{H}^+ + \text{Al}^{3+}$) suggests that higher soil acidity may act as a restrictive filter, potentially contributing to the low floristic composition observed at this site (Figure 3). Such conditions may limit recruitment and coexistence, particularly for species less tolerant of acidic and aluminum-rich substrates.

Among the analyzed attributes, soil pH emerged as one of the most relevant predictors. This trend can be explained by the role of pH in regulating nutrient availability [34,35]. Such a pattern aligns with studies reporting an association between lower soil acidity and higher aboveground biomass production [36,37], as pH directly influences the availability of essential nutrients [34,38]. At the Amazonian scale, this suggests that areas within this acidity range may function as productivity hotspots, where relatively small variations in soil chemistry induce substantial biomass responses.

Total phosphorus showed a marginal positive effect on the biomass of large trees, after which the response tended to stabilize rather than increase sharply. This pattern indicates the presence of a functional response range to phosphorus, rather than a single threshold value. The result is consistent with previous studies that identified total phosphorus as a key edaphic factor related to coarse timber production in Amazonian forests [11]. Therefore, the increase in biomass observed within this phosphorus range suggests that the soil phosphorus reservoir plays an important role in sustaining the growth of large trees under nutrient-limited conditions.

The study region lies predominantly on dystrophic Oxisols and Ultisols [39,40], typically oxidic soils characterized by low phosphorus availability, low cation-exchange capacity (CEC), and high aluminum content [31]. These conditions constrain nutrient availability and explain the strong influence of phosphorus on biomass variation. The phosphorus range identified in this study therefore represents an optimal availability window, capable of sustaining the growth of large trees even in highly weathered soils.

Aluminum exhibited a positive marginal effect on biomass within an intermediate concentration range, indicating physiological tolerance rather than simple toxicity. This response suggests adaptive mechanisms in Amazonian tree species inhabiting acidic soils. Previous studies have shown that aluminum-tolerant plants can alter cell wall composition and activate specific transporters that sequester aluminum into vacuoles, thereby reducing its toxic effects [41]. Such physiological tolerance may enhance the performance of species adapted to acidic environments, particularly light-demanding species, for which aluminum has been shown to correlate positively with growth [42]. Collectively, these findings indicate that some Amazonian tree species have developed adaptive strategies that allow them to persist and grow under acidic, aluminum-rich soil conditions.

The relationship with soil organic matter (SOM) remained relatively stable along the gradient, indicating that, despite its central role in fertility, it did not emerge as a limiting variable for biomass. SOM functions as a strategic reservoir of nutrients for both plants and microorganisms [43]. Its maintenance strongly depends on litter input and decomposition processes, which are regulated by litter quality and environmental conditions [36]. However, the dynamics of litter production and decomposition in tropical forest ecosystems are complex and still poorly understood [44]. This stability suggests that the biomass of large trees responds less to short-term fluctuations in SOM and more to long-term processes related to nutrient cycling, key mechanisms underpinning the resilience of Amazonian ecosystems.

It is important to emphasize that these results should be interpreted within the limitations of the study design. The conclusions cannot be extrapolated to the entire Amazon basin due to the restricted spatial coverage, the cluster-based sampling centered on existing large trees, and the pronounced environmental heterogeneity that characterizes Amazonian landscapes. Factors such as microtopography, hydrological regimes, disturbance history, and landscape connectivity were not explicitly addressed here and may alter edaphic-biomass relationships in other locations. Consequently, the identified patterns represent site-specific ecological responses within a recognized large tree tipping point.

4.2. Limitations and Future Research

This study advances the understanding of edaphic controls on large-tree biomass; however, it also highlights key methodological and conceptual gaps that represent important opportunities for future research.

Aboveground biomass was estimated using pantropical allometric equations, which are widely recommended for comparative tropical studies but may not fully capture local structural variability, particularly for extremely large trees. Future research integrating locally calibrated allometric models, repeated height measurements, and high-resolution terrestrial or airborne LiDAR would substantially reduce uncertainty in biomass estimates and improve representation of giant trees in carbon assessments.

Wood density values were obtained from global databases, with species- or genus-level averages applied when species-specific information was unavailable. While this approach follows current best practices, it reinforces the need for expanded field-based wood density measurements in Amazonian forests, especially for dominant and hyperdominant species that disproportionately contribute to biomass.

Plot design represents an additional challenge. The relatively small subplots used here may not fully capture the spatial extent, competitive interactions, and neighborhood effects of large trees, whose crowns and rooting systems operate at scales larger than conventional inventory units. Combining larger permanent plots with spatially explicit approaches would improve understanding of large-tree dynamics across heterogeneous landscapes.

Importantly, our results underscore a broader methodological gap: there is currently no standardized protocol specifically designed to study giant trees in Amazonian forests. Most inventory methods target average stand structure rather than the growth, mortality, and ecological role of extremely large individuals. Developing dedicated protocols for giant-tree monitoring is a critical step toward improving biomass estimates and understanding forest carbon dynamics.

In addition, hydrological processes were not explicitly assessed and may act as strong ecological filters in Amazonian landscapes. Integrating edaphic and hydrological data, along with broader site selection that includes areas where giant trees are rare or absent, will be essential for advancing a more comprehensive understanding of the factors controlling large-tree occurrence across the Amazon.

5. Conclusions

Beyond general associations, our results identify quantitative edaphic conditions linked to the biomass of large trees. Large-tree aboveground biomass increased under acidic to moderately acidic soils, particularly within a soil pH range of 3.52–6.17, at available phosphorus levels between 1.60 and 6.50 mg kg⁻¹, and within an intermediate aluminum concentration range of 0.73–1.42 cmolc kg⁻¹. These thresholds indicate that large trees are not randomly distributed along soil gradients and suggest that edaphic filtering plays an important role in structuring biomass patterns.

From a management and conservation perspective, these findings provide operationally relevant criteria for identifying areas with a higher potential to maintain large-tree populations and elevated biomass stocks. Forests occurring under these edaphic conditions may represent priority targets for conservation planning, reduced-impact logging, and restoration strategies focused on preserving structural complexity and carbon storage capacity.

In summary, the biomass of large trees in the Amazon also results from the interaction between edaphic composition and the functional responses of species along soil gradients. This relationship highlights the role of soil as a structuring component of ecological hetero-

geneity and reinforces the need to integrate edaphic parameters into predictive models and management policies aimed at conserving high-biomass tropical forests.

Author Contributions: Data curation, M.P.; Formal analysis, M.P., J.L.R.-B. and D.A.S.; Investigation, M.P., J.L.R.-B. and D.A.S.; Methodology, M.P., J.L.R.-B., D.A.S. and R.d.L.; Project administration, D.A.S. and R.d.L.; Supervision, D.A.S. and J.L.R.-B.; Writing—original draft preparation, M.P. and J.L.R.-B.; Writing—review and editing, M.P., D.A.S., J.L.R.-B., R.d.L., E.G., M.G., G.A., P.B., J.S., C.d.S., J.P.d.S. and E.d.S. All authors have read and agreed to the published version of the manuscript.

Funding: This research received no external funding. The APC will be funded by the Federal Institute of Education, Science and Technology of Amapá (IFAP).

Data Availability Statement: The raw data supporting the conclusions of this article will be made available by the authors upon reasonable request. The dataset contains precise location information of giant trees in environmentally sensitive sites, and its public release could expose these areas to risks such as unauthorized access and potential deforestation. Therefore, the dataset cannot be made openly available.

Acknowledgments: The authors thank the Long-Term Ecological Research Program: Integrated Monitoring of Amazonian Giant Trees for its scientific, logistical, and field support throughout this study. We also acknowledge the collaboration of local communities from Rio Iratapuru Sustainable Development Reserve for facilitating access to the study areas. We further thank the EMBRAPA Soil Laboratory for conducting physical and chemical analyses, and the parataxonomists who contributed to botanical identifications and the Instituto de Desenvolvimento Florestal e da Biodiversidade (Ideflor-Bio) for providing access to soil data that supported this research. The authors have reviewed and edited all generated content and take full responsibility for the final version of the manuscript.

Conflicts of Interest: The authors declare that they have no conflicts of interest.

Appendix A

The biomass of all trees and the biomass of large trees also showed significant variations among the evaluated sites, following a similar pattern (Figure A1). When comparing the two levels within each site, no statistically significant differences were observed between the mean biomass values of all trees and those of large trees alone in Urucupatá, Iratapuru, and Cupixi. This finding reinforces the idea that, in these locations, large trees account for a large proportion of the stored biomass.

The relative importance of large trees in the composition of forest biomass varied considerably among the evaluated sites. In Urucupatá, 84.3% of the total biomass of all trees was attributed to large trees, followed by Iratapuru (71.3%), Cupixi (70.0%), and Ipitinga (52.1%). These results suggest that, in some sites, large trees play a dominant role in the structure and accumulation of forest biomass.

Table A1. Summary of large-tree species (DBH \geq 70 cm) recorded in the studied Amazonian sites. For each species, we present the taxonomic family, number of individuals (N), density (individuals ha^{-1}), mean diameter at breast height (DBH \pm SD), mean height (H \pm SD), and aboveground biomass (AGB \pm SD, Mg ha^{-1}).

Species	Family	N (Individuals)	Density (ind. ha^{-1})	DBH (cm)	Height (m)	AGB (Mg ha^{-1})
<i>Andira</i> sp.	Fabaceae	1	0.167	79.6	33	0.001
<i>Aspidosperma carapanauba</i>	Apocynaceae	1	0.167	79.6	47	0.002
<i>Aspidosperma paraensis</i>	Apocynaceae	1	0.167	88.5	34	0.002
<i>Bertholletia excelsa</i>	Lecythidaceae	6	1	164.4 \pm 65.3	48 \pm 11.3	0.009 \pm 0.009

Table A1. Cont.

Species	Family	N (Individuals)	Density (ind. ha ⁻¹)	DBH (cm)	Height (m)	AGB (Mg ha ⁻¹)
<i>Bowdichia nitida</i>	Fabaceae	3	0.5	85.6 ± 17.4	20.3 ± 15	0.001 ± 0.001
<i>Bowdichia virgilioides</i>	Fabaceae	1	0.167	95.5	35	0.002
<i>Brosimum parinarioides</i>	Moraceae	2	0.333	94.7 ± 27.7	35.5 ± 3.5	0.002 ± 0.001
<i>Caryocar villosum</i>	Caryocaraceae	3	0.5	131.7 ± 54.1	37.7 ± 16.3	0.005 ± 0.005
<i>Cedrelinga cateniformis</i>	Meliaceae	2	0.333	101.1 ± 41.6	59.5 ± 7.8	0.003 ± 0.002
<i>Chrysophyllum lucentifolium</i>	Sapotaceae	1	0.167	79.6	33	0.001
<i>Corythophora rimosa</i>	Lecythidaceae	1	0.167	90.7	18	0.001
<i>Coutarea hexandra</i>	Rubiaceae	1	0.167	79.6	47	0.001
<i>Dinizia excelsa</i>	Fabaceae	4	0.667	197.8 ± 34.5	59.2 ± 16.4	0.017 ± 0.007
<i>Dipteryx odorata</i>	Fabaceae	2	0.333	130.8 ± 27.5	46.5 ± 7.8	0.006 ± 0.001
<i>Enterolobium schomburgkii</i>	Fabaceae	3	0.5	88.1 ± 18.1	37.7 ± 16.2	0.002 ± 0.000
<i>Eschweilera apiculata</i>	Lecythidaceae	2	0.333	85.9 ± 9.0	48.5 ± 2.1	0.002 ± 0.001
<i>Ficus</i> sp.	Moraceae	1	0.167	111.4	52	0.002
<i>Geissospermum sericeum</i>	Apocynaceae	1	0.167	71.6	45	0.002
<i>Goupia glabra</i>	Goupiaceae	6	1	90.2 ± 13.3	39.5 ± 9	0.002 ± 0.001
<i>Guarea carinata</i>	Meliaceae	1	0.167	75.4	46	0.001
<i>Inga auristellae</i>	Fabaceae	2	0.333	189.9 ± 160.5	43.5 ± 13.4	0.012 ± 0.015
<i>Inga</i> sp.	Fabaceae	4	0.667	176.6 ± 99.6	42.8 ± 9.1	0.009 ± 0.009
<i>Inga striata</i>	Fabaceae	1	0.167	73.2	48	0.001
<i>Laetia procera</i>	Salicaceae	1	0.167	109.8	62	0.004
<i>Lecythis lurida</i>	Lecythidaceae	1	0.167	79.6	47	0.002
<i>Manilkara paraensis</i>	Sapotaceae	2	0.333	84.4 ± 15.8	48 ± 2.8	0.003 ± 0.001
<i>Maquira sclerophylla</i>	Moraceae	1	0.167	144.8	41	0.004
<i>Minquartia guianensis</i>	Coulaceae	1	0.167	95.5	60	0.004
<i>Myrciaria floribunda</i>	Myrtaceae	5	0.833	141.2 ± 21.2	40.6 ± 2.3	0.005 ± 0.002
N.I	N.I	2	0.333	75.3 ± 6.1	39.5 ± 10.6	0.001 ± 0.001
<i>Nadenanthera peregrina</i>	Fabaceae	1	0.167	124.1	54	0.004
<i>Naucleopsis</i> sp.	Moraceae	1	0.167	157.6	42	0.006
<i>Ocotea</i> sp.	Lauraceae	1	0.167	89.1	59	0.002
<i>Parkia multijuga</i>	Fabaceae	1	0.167	102.5	36	0.001
<i>Pouteria</i> sp.	Sapotaceae	2	0.333	175.1 ± 78.8	35 ± 18.4	0.008 ± 0.009
<i>Pouteria vernicosa</i>	Sapotaceae	1	0.167	79.7	47	0.002
<i>Protium altsonii</i>	Burseraceae	4	0.667	101.7 ± 24.1	39.5 ± 5.6	0.002 ± 0.001
<i>Protium decandrum</i>	Burseraceae	2	0.333	140.5 ± 78.1	37.5 ± 10.6	0.004 ± 0.004
<i>Protium</i> sp.	Burseraceae	1	0.167	141.6	41	0.004
<i>Pseudopiptadenia suaveolens</i>	Fabaceae	4	0.667	87.3 ± 9.4	50 ± 11.9	0.002 ± 0.001
<i>Qualea paraensis</i>	Vochysiaceae	2	0.333	105.2 ± 18.2	44 ± 8.5	0.003 ± 0.000
<i>Simarouba amara</i>	Simaroubaceae	2	0.333	95.5 ± 22.5	49.5 ± 3.5	0.002 ± 0.001
<i>Swartzia polyphylla</i>	Fabaceae	1	0.167	321.5	63	0.035
<i>Tachigali myrmecophila</i>	Fabaceae	3	0.5	114.8 ± 42.6	37.7 ± 4.6	0.002 ± 0.002
<i>Terminalia amazonia</i>	Combretaceae	3	0.5	155.1 ± 110.0	53.3 ± 8.7	0.009 ± 0.011
<i>Tetragastris panamensis</i>	Burseraceae	1	0.167	70.0	11	0.000
<i>Theobroma subincanum</i>	Malvaceae	2	0.333	149.6 ± 56.3	41 ± 5.7	0.004 ± 0.003
<i>Toulicia acutifolia</i>	Sapindaceae	1	0.167	73.2	32	0.001
<i>Trattinnickia rhoifolia</i>	Burseraceae	1	0.167	80.1	33	0.001
<i>Virola</i> sp.	Myristicaceae	2	0.333	128.1 ± 21.4	47 ± 12.7	0.003 ± 0.002
<i>Virola surinamensis</i>	Myristicaceae	1	0.167	144.8	41	0.003
<i>Vochysia guianensis</i>	Vochysiaceae	1	0.167	86.9	49	0.002

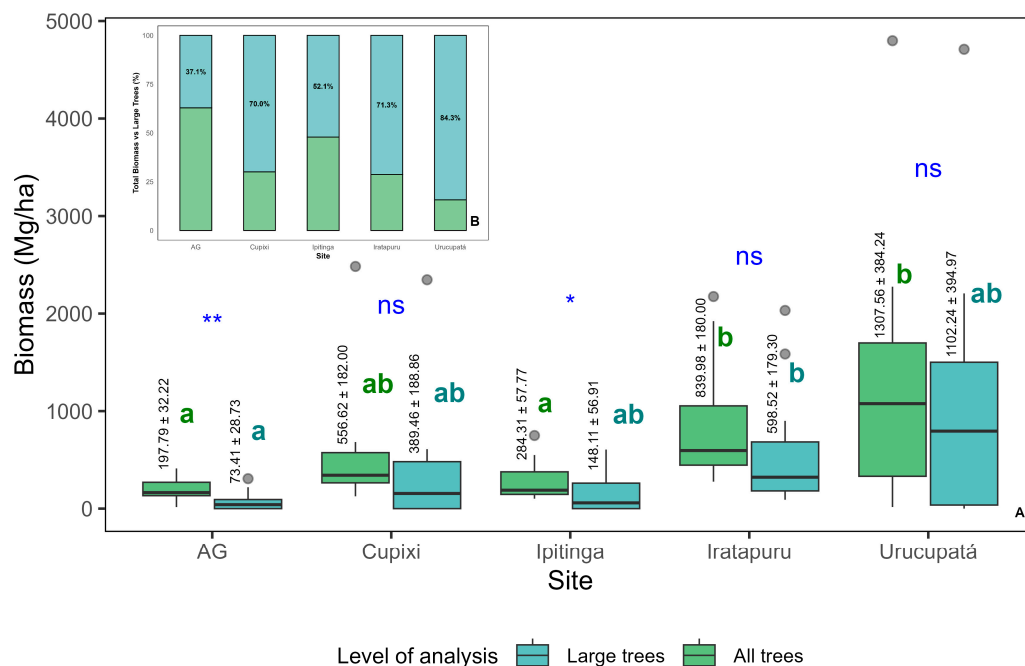


Figure A1. The biomass of all trees and that of large trees also showed significant variation among the evaluated sites, following a similar pattern. As shown in (A), the boxplots illustrate the distribution of biomass for all trees and for large trees at each site, with mean biomass values and their associated variability (standard deviation) indicated. Lowercase letters (a, b) are used to distinguish sites according to statistical differences. Asterisks indicate levels of statistical significance (* $p < 0.05$; ** $p < 0.01$), and ns indicates non-significant differences ($p \geq 0.05$). When comparing both biomass components within each site, no statistically significant differences were observed between the mean biomass of all trees and that of large trees in Urucupatá, Iratapuru, and Cupixi. (B) shows the proportion of total aboveground biomass represented by large trees, expressed as a percentage of the biomass of all trees. This finding reinforces the idea that, in these locations, large trees are responsible for a substantial share of the stored biomass.

Table A2. Mean (\pm SD) of soil chemical and physical properties across five study sites. Differences among sites were assessed using one-way ANOVA or Kruskal–Wallis χ^2 tests, with Tukey’s or Wilcoxon post hoc comparisons. Different letters indicate significant differences at 95%.

Variable	AG	Cupixi	Ipitinga	Iratapuru	Urucupatá	Statistic	p-Value
pH	4.37 ± 0.21 a	4.05 ± 0.08 b	4.36 ± 0.47 ab	4.33 ± 0.21 a	4.75 ± 1.00 a	$\chi^2 = 18.559$	<0.001
SOM	30.11 ± 8.19 a	28.92 ± 3.58 a	26.69 ± 4.30 a	16.51 ± 2.53 b	27.50 ± 4.95 a	F = 13.716	<0.001
P	2.50 ± 1.15 a	3.17 ± 4.09 ab	1.37 ± 0.59 bc	2.08 ± 0.90 ab	1.00 ± 0.23 c	$\chi^2 = 18.980$	<0.001
K	0.04 ± 0.01 a	0.02 ± 0.00 b	29.06 ± 9.09 c	0.02 ± 0.01 b	17.40 ± 5.91 d	$\chi^2 = 50.764$	<0.001
Ca_Mg	0.43 ± 0.15 a	0.08 ± 0.08 b	0.52 ± 0.53 ac	0.18 ± 0.07 cd	0.17 ± 0.15 bd	$\chi^2 = 27.973$	<0.001
Al	1.30 ± 0.25 ab	1.30 ± 0.19 ab	1.05 ± 0.57 b	1.33 ± 0.31 ab	1.60 ± 0.32 a	F = 3.790	0.009
H_Al	6.72 ± 1.44 a	7.62 ± 1.04 a	4.03 ± 0.68 b	3.93 ± 1.29 b	4.61 ± 0.61 b	F = 30.041	<0.001
CTC_pH7	7.17 ± 1.47 a	7.71 ± 1.02 a	10.97 ± 12.31 ab	4.12 ± 1.27 b	9.68 ± 8.95 ab	$\chi^2 = 23.145$	<0.001
BS	6.58 ± 2.35 ab	1.08 ± 1.16 c	28.15 ± 31.33 a	5.00 ± 2.63 b	24.34 ± 35.02 ab	$\chi^2 = 28.831$	<0.001
AS	74.08 ± 7.70 a	94.42 ± 5.20 b	52.04 ± 38.52 a	87.58 ± 5.37 c	65.50 ± 39.43 ac	$\chi^2 = 25.839$	<0.001
Clay	309.99 ± 51.33 a	460.00 ± 40.47 b	309.17 ± 140.55 a	300.08 ± 93.05 a	480.75 ± 98.37 b	$\chi^2 = 29.459$	<0.001
Coarse_Sand	337.33 ± 49.76 a	290.83 ± 30.92 a	298.58 ± 117.44 a	313.75 ± 73.10 a	255.83 ± 131.54 a	F = 1.361	0.259
Fine_Sand	124.83 ± 16.27 a	51.83 ± 15.40 b	240.08 ± 122.92 c	105.50 ± 15.80 d	174.50 ± 124.29 acd	$\chi^2 = 33.879$	<0.001
Total_Sand	462.17 ± 59.42 ab	342.67 ± 25.18 c	538.67 ± 102.64 a	419.25 ± 80.61 bc	430.33 ± 102.44 bc	F = 9.568	<0.001
Silt	227.84 ± 40.42 a	197.33 ± 33.62 a	152.17 ± 92.00 b	280.67 ± 51.09 c	88.92 ± 32.60 b	$\chi^2 = 38.387$	<0.001

Table A3. Abbreviations, full names, and measurement units of soil chemical and physical properties analyzed in the study. Chemical properties include pH, organic matter, available phosphorus, exchangeable cations, cation exchange capacity at pH, base saturation, and aluminum saturation. Physical properties correspond to soil texture fractions.

Abbreviation	Full Name	Unit
pH	Soil pH (H ₂ O)	–
SOM	Soil organic matter	g kg ^{−1}
P	Available phosphorus	mg kg ^{−1}
K	Exchangeable potassium	cmolc kg ^{−1}
Ca_Mg	Calcium + magnesium	cmolc kg ^{−1}
Al	Exchangeable aluminum	cmolc kg ^{−1}
H_Al	Potential acidity	cmolc kg ^{−1}
CTC_pH 7	Cation exchange capacity (pH 7)	cmolc kg ^{−1}
BS	Base saturation	%
AS	Aluminum saturation	%
Clay	Clay content	%
Silt	Silt content	%
Coarse_Sand	Coarse sand	%
Fine_Sand	Fine sand	%
Total_Sand	Total sand	%

Table A4. Generalized Additive Model (GAM) results for the effects of edaphic variables on the biomass of large trees (DBH ≥ 70 cm). edf = effective degrees of freedom; F_value = approximate F-statistic; p_value = significance level; Deviance_explained (%) = proportion of deviance explained by the model.

Variable	edf	F_Value	p_Value	Deviance_Explained (%)
pH	5.02	5.33	0.001	
SOM	1.00	6.82	0.014	74.6
P	2.66	5.43	0.004	
Al	4.43	4.75	0.002	

Table A5. Quantified thresholds and response patterns of edaphic variables influencing large-tree biomass derived from GAM analysis. Thresholds were identified using first-derivative analysis of the GAM smooths. Positive-response intervals correspond to ranges where the derivative was significantly greater than zero, indicating increasing large-tree biomass.

Edaphic Variable	Functional Threshold	Unit
pH	3.52–6.17	–
P	1.60–6.50	mg kg ^{−1}
Al	0.73–1.42	cmolc kg ^{−1}
SOM	No defined threshold	g kg ^{−1}

References

- Marengo, J.A.; Souza, C.M.; Thonicke, K.; Burton, C.; Halladay, K.; Betts, R.A.; Alves, L.M.; Soares, W.R. Changes in Climate and Land Use Over the Amazon Region: Current and Future Variability and Trends. *Front. Earth Sci.* **2018**, *6*, 228. [[CrossRef](#)]
- Quesada, C.A.; Paz, C.; Oblitas Mendoza, E.; Phillips, O.L.; Saiz, G.; Lloyd, J. Variations in Soil Chemical and Physical Properties Explain Basin-Wide Amazon Forest Soil Carbon Concentrations. *SOIL* **2020**, *6*, 53–88. [[CrossRef](#)]
- Pinho, B.X.; Peres, C.A.; Leal, I.R.; Tabarelli, M. Chapter Seven—Critical Role and Collapse of Tropical Mega-Trees: A Key Global Resource. In *Advances in Ecological Research*; Dumbrell, A.J., Turner, E.C., Fayle, T.M., Eds.; Tropical Ecosystems in the 21st Century; Academic Press: Cambridge, MA, USA, 2020; Volume 62, pp. 253–294.
- Enquist, B.J.; Abraham, A.J.; Harfoot, M.B.J.; Malhi, Y.; Doughty, C.E. The Megabiota Are Disproportionately Important for Biosphere Functioning. *Nat. Commun.* **2020**, *11*, 699. [[CrossRef](#)] [[PubMed](#)]

5. de Lima, R.B.; Görgens, E.B.; da Silva, D.A.S.; de Oliveira, C.P.; Batista, A.P.B.; Caraciolo Ferreira, R.L.; Costa, F.R.C.; Ferreira de Lima, R.A.; da Silva Aparício, P.; de Abreu, J.C.; et al. Giants of the Amazon: How Does Environmental Variation Drive the Diversity Patterns of Large Trees? *Glob. Change Biol.* **2023**, *29*, 4861–4879. [[CrossRef](#)]
6. de Lima, R.B.; da Silva, D.A.S.; Nunes, M.H.; de Lima Bittencourt, P.R.; Groenendijk, P.; de Oliveira, C.P.; de Souza, D.G.; Ferreira, R.L.C.; da Silva, J.A.A.; Aguirre-Gutiérrez, J.; et al. Mapping Giant-Tree Density in the Amazon. *bioRxiv* **2025**. [[CrossRef](#)]
7. Harris, D.J.; Ndolo Ebika, S.T.; Sanz, C.M.; Madingou, M.P.N.; Morgan, D.B. Large Trees in Tropical Rain Forests Require Big Plots. *Plants People Planet* **2021**, *3*, 282–294. [[CrossRef](#)]
8. Slik, J.W.F.; Paoli, G.; McGuire, K.; Amaral, I.; Barroso, J.; Bastian, M.; Blanc, L.; Bongers, F.; Boundja, P.; Clark, C.; et al. Large Trees Drive Forest Aboveground Biomass Variation in Moist Lowland Forests across the Tropics. *Glob. Ecol. Biogeogr.* **2013**, *22*, 1261–1271. [[CrossRef](#)]
9. Bradford, M.; Murphy, H.T. The importance of large-diameter trees in the wet tropical rainforests of Australia. *PLoS ONE* **2019**, *14*, e0208377. [[CrossRef](#)]
10. Gorgens, E.B.; Motta, A.Z.; Assis, M.; Nunes, M.H.; Jackson, T.; Coomes, D.; Rosette, J.; Aragão, L.E.O.E.C.; Ometto, J.P. The Giant Trees of the Amazon Basin. *Front. Ecol. Environ.* **2019**, *17*, 373–374. [[CrossRef](#)]
11. Quesada, C.A.; Phillips, O.L.; Schwarz, M.; Czimczik, C.I.; Baker, T.R.; Patiño, S.; Fyllas, N.M.; Hodnett, M.G.; Herrera, R.; Almeida, S.; et al. Basin-Wide Variations in Amazon Forest Structure and Function Are Mediated by Both Soils and Climate. *Biogeosciences* **2012**, *9*, 2203–2246. [[CrossRef](#)]
12. Draper, F.C.; Costa, F.R.C.; Arellano, G.; Phillips, O.L.; Duque, A.; Macía, M.J.; ter Steege, H.; Asner, G.P.; Berenguer, E.; Schiatti, J.; et al. Amazon Tree Dominance across Forest Strata. *Nat. Ecol. Evol.* **2021**, *5*, 757–767. [[CrossRef](#)]
13. Fauset, S.; Johnson, M.O.; Gloor, M.; Baker, T.R.; Monteagudo, M.A.; Brienen, R.J.W.; Feldpausch, T.R.; Lopez-Gonzalez, G.; Malhi, Y. Hyperdominance in Amazonian Forest Carbon Cycling. *Nat. Commun.* **2015**, *6*, 6857. [[CrossRef](#)] [[PubMed](#)]
14. Lutz, J.A.; Furniss, T.J.; Johnson, D.J.; Davies, S.J.; Allen, D.; Alonso, A.; Anderson-Teixeira, K.J.; Andrade, A.; Baltzer, J.; Becker, K.M.L.; et al. Global Importance of Large-Diameter Trees. *Glob. Ecol. Biogeogr.* **2018**, *27*, 849–864. [[CrossRef](#)]
15. Carvalho, R.L.; Resende, A.F.; Barlow, J.; França, F.M.; Moura, M.R.; Maciel, R.; Alves-Martins, F.; Shutt, J.; Nunes, C.A.; Elias, F.; et al. Pervasive Gaps in Amazonian Ecological Research. *Curr. Biol.* **2023**, *33*, 3495–3504. [[CrossRef](#)]
16. Alvares, C.A.; Stape, J.L.; Sentelhas, P.C.; Leonardo, J.; Gonçalves, M.; Sparovek, G. Köppen’s Climate Classification Map for Brazil. *Meteorol. Z.* **2013**, *26*, 711–728. [[CrossRef](#)]
17. IFN—Metodologia—Serviço Florestal Brasileiro. Available online: <https://www.gov.br/florestal/pt-br/assuntos/ifn/metodologia> (accessed on 31 December 2025).
18. Coelho, A.M. Amostragem de Solos: A base para aplicação de corretivos e fertilizantes. In *Embrapa Milho e Sorgo. Comunicado Técnico*; Embrapa Milho e Sorgo: Sete Lagoas, Brazil, 2003; p. 73.
19. Guarçoni, A.; Alvarez V, V.H.; Sobreira, F.M.; Guarçoni, A.; Alvarez V, V.H.; Sobreira, F.M. Fundamentação teórica dos sistemas de amostragem de solo de acordo com a variabilidade de características químicas. *Terra Latinoam.* **2017**, *35*, 343–352. [[CrossRef](#)]
20. Teixeira, P.C.; Donagemma, G.K.; Fontana, A.; Teixeira, W.G. *Manual de Métodos de Análise de Solo*; Embrapa Solos: Rio de Janeiro, Brazil, 2017.
21. Réjou-Méchain, M.; Tanguy, A.; Piponiot, C.; Chave, J.; Hérault, B. Biomass: An R Package for Estimating above-Ground Biomass and Its Uncertainty in Tropical Forests. *Methods Ecol. Evol.* **2017**, *8*, 1163–1167. [[CrossRef](#)]
22. Chave, J.; Réjou-Méchain, M.; Búrquez, A.; Chidumayo, E.; Colgan, M.S.; Delitti, W.B.C.; Duque, A.; Eid, T.; Fearnside, P.M.; Goodman, R.C.; et al. Improved Allometric Models to Estimate the Aboveground Biomass of Tropical Trees. *Glob. Change Biol.* **2014**, *20*, 3177–3190. [[CrossRef](#)]
23. Legendre, P.; Legendre, L. *Numerical Ecology*; Elsevier: Amsterdam, The Netherlands, 2012; ISBN 978-0-444-53869-7.
24. Legendre, P.; Gallagher, E.D. Ecologically Meaningful Transformations for Ordination of Species Data. *Oecologia* **2001**, *129*, 271–280. [[CrossRef](#)] [[PubMed](#)]
25. Dray, S.; David, B.; Guillaume, B.; Daniel, B.; Sylvie, C.; Guillaume, G. *Adespatial: Multivariate Multiscale Spatial Analysis 0.3-28*; R Foundation for Statistical Computing: Vienna, Austria, 2016.
26. Oksanen, J.; Blanchet, F.; Friendly, M.; Kindt, R. *Vegan: Community Ecology Package (R Package Version 2.5–5)*, 2019.
27. Burnham, K.P.; Anderson, D.R. (Eds.) Advanced Issues and Deeper Insights. In *Model Selection and Multimodel Inference: A Practical Information-Theoretic Approach*; Springer: New York, NY, USA, 2002; pp. 267–351, ISBN 978-0-387-22456-5.
28. Team R Core R. *The R Project for Statistical Computing*; R Foundation for Statistical Computing: Vienna, Austria, 2024.
29. Wood, S. *Generalized Additive Models: An Introduction With R*; CRC Press: Boca Raton, FL, USA, 2017.
30. Guisan, A.; Zimmermann, N.E. Predictive Habitat Distribution Models in Ecology. *Ecol. Model.* **2000**, *135*, 147–186. [[CrossRef](#)]
31. Stephenson, N.L.; Das, A.J.; Condit, R.; Russo, S.E.; Baker, P.J.; Beckman, N.G.; Coomes, D.A.; Lines, E.R.; Morris, W.K.; Rüger, N.; et al. Rate of Tree Carbon Accumulation Increases Continuously with Tree Size. *Nature* **2014**, *507*, 90–93. [[CrossRef](#)]

32. Luizão, F.J.; Fearnside, P.M.; Cerri, C.E.P.; Lehmann, J. The Maintenance of Soil Fertility in Amazonian Managed Systems. In *Geophysical Monograph Series*; Keller, M., Bustamante, M., Gash, J., Silva Dias, P., Eds.; American Geophysical Union: Washington, DC, USA, 2009; Volume 186, pp. 311–336, ISBN 978-0-87590-476-4.
33. Quesada, C.; Lloyd, J.; Schwarz, M.; Patiño, S.; Baker, T.R.; Czimczik, C.; Paiva, R. Variations in Chemical and Physical Properties of Amazon Forest Soils in Relation to Their Genesis. *Biogeosciences* **2010**, *7*, 1515–1541. [[CrossRef](#)]
34. Sayer, E.J.; Banin, L.F. Tree Nutrient Status and Nutrient Cycling in Tropical Forest—Lessons from Fertilization Experiments. *Trop. Tree Physiol.* **2016**, *6*, 275–297. [[CrossRef](#)]
35. McCauley, A.; Jones, C.; Jacobsen, J. Soil pH and Organic Matter. *Nutr. Manag. Modul.* **2009**, *8*, 1–12.
36. Poggio, L.; de Sousa, L.M.; Batjes, N.H.; Heuvelink, G.B.M.; Kempen, B.; Ribeiro, E.; Rossiter, D. SoilGrids 2.0: Producing Soil Information for the Globe with Quantified Spatial Uncertainty. *SOIL* **2021**, *7*, 217–240. [[CrossRef](#)]
37. van der Sande, M.T.; Arets, E.J.M.M.; Peña-Claros, M.; Hoosbeek, M.R.; Cáceres-Siani, Y.; van der Hout, P.; Poorter, L. Soil Fertility and Species Traits, but Not Diversity, Drive Productivity and Biomass Stocks in a Guyanese Tropical Rainforest. *Funct. Ecol.* **2018**, *32*, 461–474. [[CrossRef](#)]
38. Hornink, B.; Zuidema, P.A.; van der Sleen, P.; Zanne, A.E.; Assis-Pereira, G.; Ortega Rodriguez, D.R.; Fontana, C.; Portal-Cahuana, L.A.; Requena-Rojas, E.J.; Barbosa, A.C.M.C.; et al. Biomass Production of Tropical Trees across Space and Time: The Shifting Roles of Diameter Growth and Wood Density. *J. Ecol.* **2025**, *113*, 3141–3158. [[CrossRef](#)]
39. Isa, N.; Razak, S.A.; Abdullah, R.; Khan, M.N.; Hamzah, S.N.; Kaplan, A.; Dossou-Yovo, H.O.; Ali, B.; Razzaq, A.; Wahab, S.; et al. Relationship between the Floristic Composition and Soil Characteristics of a Tropical Rainforest (TRF). *Forests* **2023**, *14*, 306. [[CrossRef](#)]
40. Brazilian Institute of Geography and Statistics—IBGE Amapá—Mapa Exploratório de Solos Em Escala 1:5.000.000. Available online: https://geoftp.ibge.gov.br/informacoes_ambientais/pedologia/mapas/unidades_da_federacao/ap_pedologia.pdf (accessed on 14 November 2025).
41. Brazilian Institute of Geography and Statistics—IBG Pará—Mapa Exploratório de Solos Em Escala 1:5.000.000. Available online: https://geoftp.ibge.gov.br/informacoes_ambientais/pedologia/mapas/ (accessed on 14 November 2025).
42. Kochian, L.V.; Piñeros, M.A.; Liu, J.; Magalhaes, J.V. Plant Adaptation to Acid Soils: The Molecular Basis for Crop Aluminum Resistance. *Annu. Rev. Plant Biol.* **2015**, *66*, 571–598. [[CrossRef](#)]
43. Reategui-Betancourt, J.L.; de Freitas, L.J.M.; Nascimento, R.G.M.; Briceño, G.; Figueiredo, A.E.S.; Rezende, A.V.; Alder, D. Species Grouping and Diameter Growth of Trees in the Eastern Amazon: Influence of Environmental Factors after Reduced-Impact Logging. *For. Ecol. Manag.* **2025**, *578*, 122465. [[CrossRef](#)]
44. Lange, D.F.; Schröter, S.A.; da Luz, F.M.; Pires, E.; Santos, Y.R.; da Silva, J.S.; Hildmann, S.; Hoffmann, T.; Ferreira, S.J.F.; Schäfer, T.; et al. Cycling of Dissolved Organic Nutrients and Indications for Nutrient Limitations in Contrasting Amazon Rainforest Ecosystems. *Biogeochemistry* **2024**, *167*, 1567–1588. [[CrossRef](#)]

Disclaimer/Publisher’s Note: The statements, opinions and data contained in all publications are solely those of the individual author(s) and contributor(s) and not of MDPI and/or the editor(s). MDPI and/or the editor(s) disclaim responsibility for any injury to people or property resulting from any ideas, methods, instructions or products referred to in the content.